Interfacial fracture toughness of GaN film on diamond substrate for application in ultra-high power RF devices

Dong Liu*, Stephen Fabes, Daniel Francis, and Martin Kuball
Center for Device Thermography and Reliability (CDTR), University of Bristol, Bristol, BS8 1TL, UK

Corresponding email: dong.liu@bristol.ac.uk; Tel. +44 (0) 117 928 8702

Keywords: GaN-on-diamond, Nanoindentation, Interfacial toughness, Thermal boundary resistance, Transient thermoreflectance.

Abstract

Achieving a mechanically stable interface with low thermal boundary resistance in GaN-on-diamond is crucial for reliable operation of high-power devices . As one cannot grow diamond directly to GaN due to crystallographic restrictions, an interlayer of SiN_x is usually introduced between GaN and diamond. This layer not only affects the thermal resistance of the heterogeneously integrated GaN-on-diamond material, but also impact its mechanical strength. In this work, a series of GaN-on-diamond materials with varying SiN_x thicknesses were studied. First of all, the GaN/diamond interfacial toughness was measured by nano-indentation. Secondly, the effective thermal boundary resistance was evaluated by transient thermoreflectance method. In addition, to understand the complex stress-strain field at the interface, a 2D axisymmetric finite element model has been established and validated by experimental results. It was found that the reduction in SiN_x interlayer thickness benefits the thermal properties of GaN-on-diamond without compromising its mechanical stability.

INTRODUCTION

Over the past decade, GaN-based high electron mobility transistors (HEMTs) have made great contributions for high-power radio frequency (RF) applications. However, the reliability and integrity of these GaN-based devices were predominately limited by their non-optimal heat removal capability. To tackle this problem, diamond substrates with high thermal conductivity and good heat spreading capability have been integrated with GaN films to produce GaN-on-diamond electronics [1]. More than three times higher power density can be achieved using GaN-on-diamond devices compared with the conventional GaN-on-SiC devices [2]. Although the thermal management has been improved, in recent years, there has been a concern about the mechanical stability of the GaN/diamond interface prior to and during device operation. Several researchers have proposed micro-mechanical methods to evaluate the interfacial stability of GaN-on-diamond materials [3][4]. Nevertheless, there has been no systematic quantification of the interfacial strength/toughness in GaN-on-diamond materials processed with varying parameters.

Here, nanoindentation and transient thermoreflectance (TTR) methods were used to assess the interfacial mechanical strength and the effective thermal boundary resistance (TBR_{eff}) of seven GaN-on-diamond materials, respectively, with the aim to establish the relationships between processing parameters, interfacial strength and TBR_{eff}.

EXPERIMENT

The GaN-on-diamond materials studied were fabricated using the double-flip process described in refs. [1][5]. An AlGaN/GaN heterostructure layer was first grown on silicon substrate using metal organic chemical vapour deposition (MOCVD). The GaN-epilayer structure was then attached to a handling wafer, after which the strain relief layer and the original growth silicon substrate were removed. A thin dielectric SiN_x interlayer was subsequently deposited onto the exposed GaN film to enhance diamond seeding before the growth of a ~100 μm polycrystalline diamond substrate.

In this work, seven types of GaN-on-diamond materials were studied in total, with varying thickness of GaN film (500~850 nm) and SiN_x interlayer (17~70 nm). In addition, GaN (1800 nm)-on-sapphire and GaN (1500 nm)-on-SiC materials were also measured for comparison. For all the samples, the interfacial toughness was evaluated using a Hysitron TI Premier nanoindenter. During the experiment, a maximum load of 350 mN was applied to the top surface of GaN using a Berkovich diamond indenter under a constant loading rate of 10 nm/s to create a local delamination at the interface. In order to obtain a statistic result, in excess of 40 indentation tests were performed for each sample. The indents were set 30-40 μm apart from each other to avoid any interactions between these indents. Further, the geometry of the delaminated area (diameter and height) was measured by a Bruker Dimension Edge atomic force microscope (AFM). The delamination/crack formed at

the GaN/diamond interface was investigated by focus ion beam milling (FIB) and scanning electron microscope (SEM) imaging at a sample tilt of 52 degrees. Subsequently, a 2D axisymmetric finite element (FE) model was implemented in ANSYS to understand the complex stress and strain field produced during the indentation process (no delamination). The TBR_{eff} at GaN/diamond interface was measured by the TTR method, where a 1ns 355 nm pump laser (frequency-tripled Nd:YAG laser) was used to heat the sample surface. The change of the linearly temperature-dependent surface reflectance in the time domain was detected using a 462 nm probe beam. More details of this technique can be found in refs. [6][7]. The results were correlated to the interfacial toughness of GaN-on-diamond.

RESULTS AND DISCUSSION

Arrays of indents have been introduced to GaN layer, as indicated in Fig.1. The circular area around the indent impression indicates the formation of interfacial delamination which was found to initiate when indentation depth was close to the GaN film thickness in all GaN-on-diamond and the GaN-on-sapphire materials. No noticeable delamination was formed in the GaN-on-SiC. Based on the load applied and the geometry of the delamination, the interfacial toughness of the interface was determined using two analytical models: 'Hutchinson and Suo model' [8] and 'Dual-indentation model' [9]. The Hutchinson and Suo model evaluates the interfacial toughness by measuring the geometry of the blisters while the Dual-indentation model derived the interfacial toughness from the indentation load-depth curve.

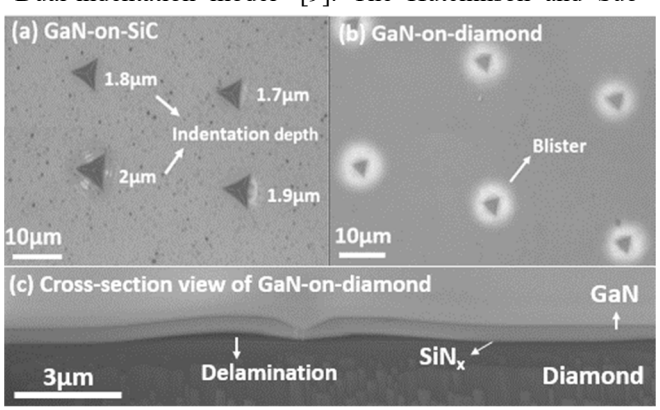

Fig. 1. Optical images of GaN surface in (a) GaN-on-SiC and (b) GaN-on-diamond; (c) SEM image of GaN-on-diamond cross-section after the indentation test, with no delamination achieved on GaN-on-SiC and with delamination on GaN-on-diamond.

The value of the interfacial toughness evaluated by the two analytical models are consistent. In general, the interface between GaN and diamond is expectedly weaker than GaN/sapphire and GaN/SiC interfaces. For example, the interfacial toughness is 0.76-1.26 J/m^2 for GaN-on-diamond and around 3 ± 0.3 J/m^2 for the GaN-on-sapphire.

The interfaces in the as-made GaN-on-diamond materials were found to be free from microscopic defects (Fig.2a). The GaN/SiN_x interface was generally flat and smooth while a waved interface can be seen between SiN_x and diamond. Delamination within GaN-on-diamond was found to initiate and propagate preferably along the SiN_x/diamond interface. Small residual SiN_x pieces were found distributing randomly around the delaminated area on the diamond seeding surface.

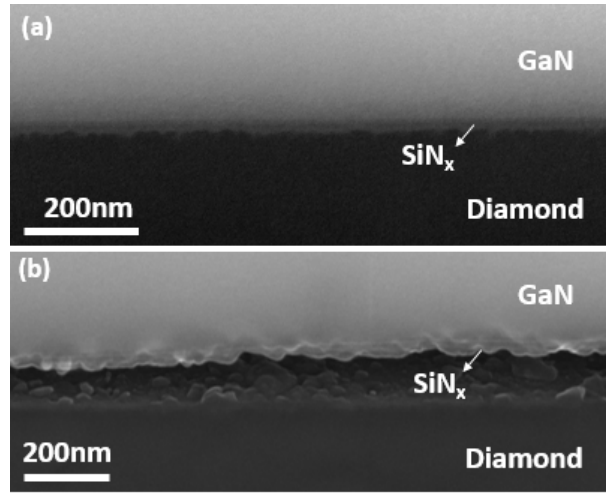

Fig. 2. Cross-sectional SEM image of GaN-on-diamond (a) before and (b) after delamination.

The TBR_{eff} for the GaN-on-diamond interface was measured to be 14-28 m^2K/GW, which is higher than the predicted value for a perfect GaN/diamond interface without any interlayer [10]. The lowest TBR_{eff} value (14 ± 1 m^2K/GW) was obtained for the GaN-on-diamond with the thinnest SiN_x interlayer (17 nm), which is consistent with the results from Sun et al. [7]. It is worth noting that, the mechanical interfacial toughness of GaN-on-diamond was not compromised by the reduction of the SiN_x thickness.

To further understand the stress distribution in the GaN film and at GaN/diamond interfaces, a nano-indentation process (no delamination) was simulated by FE (Fig. 3). A conical indenter with the same projected area-depth function as Berkovich indenter was used and the indenter tip radius was taken into account. The friction coefficient between the tip and the specimen surface was assumed to be zero and the interfaces perfectly bonded. All layers in the simulation were defined as bilinear elastic-plastic materials with isotropic elasticity.

The simulated load-depth curve showed good agreement with the experimental data. The stress field within the material expands vertically and laterally around the indenter

tip as the indentation depth increases. Discontinuities of stress/strain field were found at the interfaces (Fig.4.).

It is clearly evident that the difference in equivalent (Von-Mises) elastic strain between SiN_x and diamond is larger than that between GaN and SiN_x. This indicates that, theoretically, the SiN_x/diamond interface is more vulnerable and prone to be the delaminated interface with a certain load/pressure applied on the GaN surface, which is consistent with the experimental observations. This model will be used for future analysis of the interfacial delamination process.

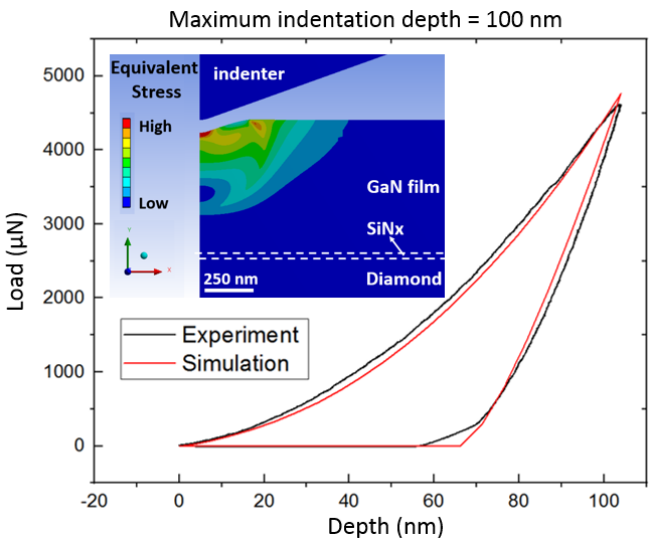

Fig. 3. Experimentally measured and FE simulated load-depth curve of a nanoindentation process (no delamination) on a GaN-on-diamond material, with maximum indentation depth of 100nm. Insert shows the corresponding equivalent (Von-Mises) stress distribution.

CONCLUSIONS

1. The interfacial toughness of different GaN systems showed the following order:
   GaN-on-diamond < GaN-on-sapphire < GaN-on-SiC.
2. The GaN-on-diamond materials showed both good interfacial toughness and low thermal resistance.
3. The reduction in the thickness of SiN_x is beneficial to the thermal management within GaN-on-diamond materials, without compromising the interfacial mechanical stability.
4. The nano-indentation process (no delamination) simulated by the 2D FE model produced consistent load-depth curve as the experimental data. The SiN_x/diamond interface was found to be under higher stress/strain state compared with the GaN/diamond interface during the indentation test.

ACKNOWLEDGEMENTS

This work was in part supported by the UK Engineering and Physical Science Research Council (EPSRC) under the Program Grant GaN-DaME (EP/P00945X); CL acknowledged partial financial support by Element Six Technologies for her studentship, DL acknowledges EPSRC Research Fellowship project (EP/N004493/1) and the Royal Commission for the Exhibition of 1851 Brunel Research Fellowship funding. The authors are grateful to Dr Filip Gucmann (University of Bristol) for the FIB cutting and taking the SEM micrographs. We thank Element Six Technologies for providing the samples for this study.

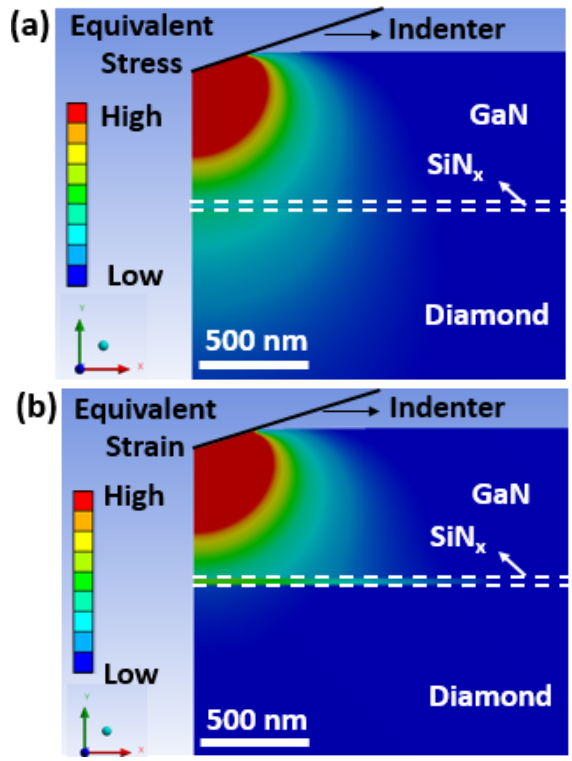

Fig. 4. Equivalent (Von-Mises) (a) stress and (b) elastic strain distribution within GaN-on-diamond when indentation depth reaches 15% of the GaN film thickness.

REFERENCES

[1] D. Francis, J. Wasserbauer, and F. Faili, *Proc. CS MANTECH, Austin, TX*, no. 650, p. 133, 2007.

[2] J. W. Pomeroy, M. Bernardoni, D. C. Dumka, D. M. Fanning, and M. Kuball, *Appl. Phys. Lett.*, vol. 104, no. 8, pp. 1–6, 2014.

[3] D. Liu, D. Francis, F. Faili, C. Middleton, J. Anaya, J. W. Pomeroy, D. J. Twitchen, and M. Kuball, *Scr. Mater.*, vol. 128, pp. 57–60, 2016.
[4] D. Liu, H. Sun, J. W. Pomeroy, D. Francis, F. Faili, D. J. Twitchen, and M. Kuball, Appl. Phys. Lett., vol. 107, no. 25, 2015.
[5] D. Francis, F. Faili, D. Babić, F. Ejeckam, A. Nurmikko, and H. Maris, Diam. Relat. Mater., vol. 19, no. 2–3, pp. 229–233, 2010.
[6] J.W.Pomeroy, R. B. Simon, H. Sun, D.Francis, F. Faili, D. J. Twitchen, and M. Kuball, IEEE Electron Device Lett., vol. 35, no. 10, 2014.
[7] H. Sun, R. B. Simon, J. W. Pomeroy, D. Francis, F. Faili, D. J. Twitchen, and M. Kuball, Appl. Phys. Lett., vol. 106, no. 11, 2015.
[8] J. W. Hutchinson, "Mixed Mode Cracking in Layered Materials," Adv. in Appl. Mech. vol. 29. 1992.
[9] M. Lu and H. Huang, J. Mater. Res., vol. 29, no. 6, pp. 801–810, 2014.
[10] P. Reddy, K. Castelino, and A. Majumdar, Appl. Phys. Lett., vol. 87, no. 21, pp. 1–3, 2005.

ACRONYMS

HEMT: High Electron Mobility Transistor
RF: Radio Frequency
TTR: Transient Thermoreflectance
TBReff : Effective Thermal Boundary Resistance
MOCVD: Metal Organic Chemical Vapour Deposition
AFM: Atomic Force Microscope
FIB: Focused Ion Beam
SEM: Scanning Electron Microscope
FE: Finite Element